

## Functional Complementation of Nuclear Targeting-Defective Mutants of Simian Virus 40 Structural Proteins

NORIO ISHII, AKIRA NAKANISHI, MASAYASU YAMADA,†  
MICHAEL H. MACALALAD, AND HARUMI KASAMATSU\*

*Department of Biology and Molecular Biology Institute, University of California,  
Los Angeles, Los Angeles, California 90024*

Received 25 May 1994/Accepted 7 September 1994

**Structural proteins of simian virus 40 (SV40), Vp2 and Vp3 (Vp2/3) and Vp1, carry individual nuclear targeting signals, Vp3<sub>198–206</sub> (Vp2<sub>316–324</sub>) and Vp1<sub>1–8</sub>, respectively, which are encoded in different reading frames of an overlapping region of the genome. How signals coordinate nuclear targeting during virion morphogenesis was examined by using SV40 variants in which there is only one structural gene for Vp1 or Vp2/3, nuclear targeting-defective mutants thereof, Vp2/3<sub>202T</sub> and Vp1ΔN5, or nonoverlapping SV40 variants in which the genes for Vp1 and Vp2/3 are separated, and mutant derivatives of the gene carrying either one or both mutations. Nuclear targeting was assessed immunocytochemically following nuclear microinjection of the variant DNAs. When Vp2/3 and Vp1 mutants with defects in the nuclear targeting signals were expressed individually, the mutant proteins localized mostly to the cytoplasm. However, when mutant Vp2/3<sub>202T</sub> was coexpressed in the same cell along with wild-type Vp1, the mutant protein was effectively targeted to the nucleus. Likewise, the Vp1ΔN5 mutant protein was transported into the nucleus when wild-type Vp2/3 was expressed in the same cells. These results suggest that while Vp1 and Vp2/3 have independent nuclear targeting signals, additional signals, such as those defining protein-protein interactions, play a concerted role in nuclear localization along with the nuclear targeting signals of the individual proteins.**

During the late phase of simian virus 40 (SV40) infection, cytoplasmically synthesized structural proteins, Vp1, Vp2, and Vp3, are transported into the nucleus within 60 min of their synthesis (23), where they assemble into mature virions with SV40 minichromosomes (28). The fine structure of SV40 reveals that the virion is composed of 72 Vp1 pentamers (1, 21), each of which is presumed to interact with one molecule of either Vp2 or Vp3 (1, 21). Since the formation of SV40 Vp1 pentamers occurs *in vitro* (16), pentamer formation can also be expected to occur in the cytoplasm soon after synthesis during SV40 infection. The site at which Vp2 and Vp3 interact with Vp1 following synthesis is not known. They might be transported individually to the nucleus, or they might interact in the cytoplasm. On the basis of genetic and biochemical data, we have proposed that the viral structural proteins destined to form the mature virion in the nucleus interact in the cytoplasm (19, 22). As the structural proteins are known to carry individual nuclear targeting signals (as discussed below) which are responsible for their nuclear localization following their synthesis (7, 15, 17, 29, 30), this hypothesis can be tested experimentally. The phenotypic rescue of the targeting-defective Vp1, for example, is expected to occur when Vp2 or Vp3 is present.

Three structural proteins of SV40 are encoded in a partially overlapping manner on the genome. The genes of the minor structural proteins, Vp2 and Vp3 (herein designated Vp2/3), are translated in the same reading frame, with the amino acid sequence of Vp3 corresponding to the carboxy-terminal two-thirds of Vp2. The gene for the major coat protein, Vp1, begins 38 codons 5' to the Vp2/3 termination codon and is translated

in a different reading frame. Within the carboxy-terminal 35 residues of Vp2/3, there exist a DNA-binding domain (6) and a Vp1-interactive determinant (15), in addition to the Vp2/3 nuclear transport signal (NTS) which maps to residues 198 to 206 of Vp3 (316 to 324 of Vp2). The Vp2/3 NTS is necessary and sufficient to target the proteins to the nucleus (7, 9). The nuclear localization signal (NLS) of Vp1 has been mapped by deletion analysis of poliovirus Vp1-SV40 Vp1 fusion proteins to the amino-terminal eight residues of Vp1 (29), yet it cannot function as an independent NTS. When these residues were conjugated at the carboxy terminus to chicken serum albumin, they were unable to promote entry of the nonnuclear protein into the nucleus (5). How these two different signals, Vp2/3-NTS and Vp1-NLS, function in the nuclear targeting of the viral proteins is not well understood; hence, we refer to them as nuclear targeting signals. Both targeting signals are within the overlapping region. As mutations in the overlapping region of Vp2/3 could inevitably introduce alterations in the Vp1 sequence, we constructed a nonoverlapping SV40 (NO-SV40), whose Vp2/3 genes are separated from the Vp1 gene. In this study, we have tested for the complementation of the nuclear targeting-defective Vp1 (or Vp2/3) by Vp2/3 (or Vp1).

### MATERIALS AND METHODS

**Plasmid construction.** The strategy of the construction of the plasmids used in this study is diagrammed in Fig. 1. All DNA manipulations were performed as described previously (25).

pSV40 containing the wild-type SV40 DNA inserted into pBR322 as a shuttle vector has been described earlier (16).

pSV-Vp1, in which the Vp2 and Vp3 coding sequences were deleted from pSV40, was constructed by ligating a 6.9-kb *KpnI*-*Bpu*1102I fragment and a 263-bp *KpnI*-*Ava*II fragment from pSV40 with a 225-bp *Ava*II-*Bpu*1102I fragment synthesized by PCR. The 225-bp fragment, which lacks most of the

\* Corresponding author. Mailing address: Department of Biology, University of California, Los Angeles, 405 Hilgard Ave., Los Angeles, CA 90024. Phone: (310) 825-3048. Fax: (310) 206-7286.

† Present address: Department of Animal Science, College of Agriculture, Kyoto University, Kyoto 606, Japan.

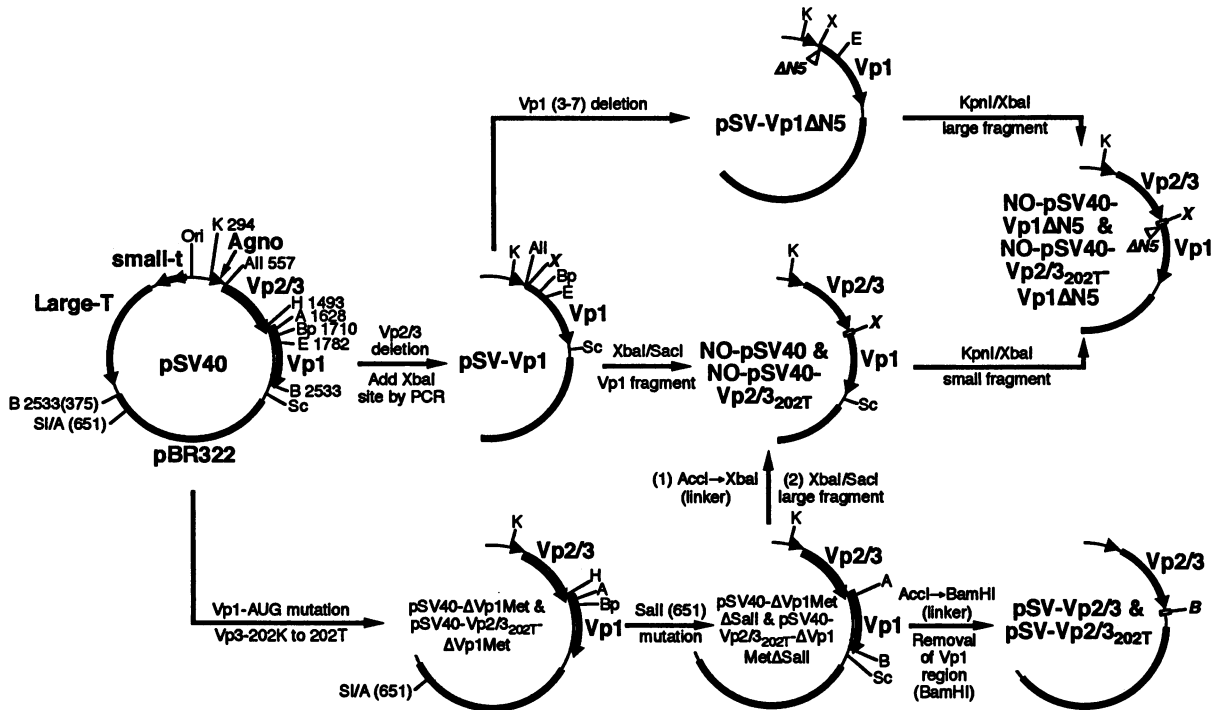


FIG. 1. Construction of SV40 and NO-SV40 variant plasmid DNAs. A schematic diagram for the construction of pSV-Vp1, pSV-Vp1 $\Delta$ N5, pSV-Vp2/3, pSV-Vp2/3<sub>202T</sub>, NO-pSV40, NO-pSV40-Vp1 $\Delta$ N5, NO-pSV40-Vp2/3<sub>202T</sub>, and NO-pSV40-Vp2/3<sub>202T</sub>-Vp1 $\Delta$ N5 is presented. All of the constructs as well as the intermediate plasmids encode SV40 large T antigen (Large-T), small t antigen (small-t), and agnoprotein (agno) and harbor all the regulatory elements (as shown for pSV40). Only the pertinent portion of each plasmid is shown. The location for the deletion of the third to seventh residues of Vp1 is marked by a  $\Delta$ N5. The numbers represent the SV40 nucleotide numbers, and those in parentheses are those of pBR322. Abbreviations: Ori, origin of replication; A, *AccI*; AII, *AvaII*; B, *BamHI*; Bp, *Bpu1102I*; E, *EcoRI*; H, *HindIII*; K, *KpnI*; Sc, *SacI*; S, *SalI*; X, *XbaI*.

Vp2/3 region (SV40 nucleotides [nt] 567 to 1498), was generated by using pSV40 as a template and then digested with *AvaII* and *Bpu1102I*. The sense primer, 5'-GTCCTTTTATTTTCAGGTCCATGGTCTAGATGAAGATGGCCCCAACAA-3', represents the SV40 sequence upstream of nt 567 and downstream of nt 1948, and also includes an *XbaI* site (underlined) upstream of the start codon of Vp1 (boldface letters) to facilitate subsequent manipulation. The antisense primer, 5'-CAAAGGAATTCTAGCCACACTGTAGCA-3', represents the SV40 sequence from nt 1792 to 1766.

pSV-Vp1 $\Delta$ N5 contains a 5-amino-acid deletion of residues 3 through 7 of Vp1, and was constructed by exchanging a 288-bp *XbaI-EcoRI* fragment of pSV-Vp1 for a PCR-generated 273-bp *XbaI-EcoRI* fragment. The 273-bp fragment containing the designated deletion was generated by using pSV-Vp1 as a template and digested by *XbaI* and *EcoRI*. The sense primer was 5'-TGCTCTAGATGAAGATGGCCGGAAGTTGTCCAGGGGCA-3' (nt 563 to 1543 with deletion of Vp2/3 coding sequences), and the antisense primer was as described above.

pSV-Vp2/3, in which only the Vp2/3 structural gene is present, and pSV-Vp2/3<sub>202T</sub>, in which lysine 202 of Vp3 is mutated to threonine, were generated from pSV40- $\Delta$ Vp1Met and pSV40<sub>202T</sub>- $\Delta$ Vp1Met, respectively. Briefly, *KpnI-Bpu1102I*, 6.9- and 1.4-kb fragments of pSV40 were separated and the 1.4-kb fragment was partially digested with *HindIII* to yield a 1.2-kb *KpnI-HindIII* fragment. The 6.9- and 1.2-kb fragments were ligated together with a 217-bp mutated PCR fragment to generate pSV40- $\Delta$ Vp1Met and pSV40<sub>202T</sub>- $\Delta$ Vp1Met, respectively. In these plasmids, two ATG codons at the

Vp1 start region were eliminated by substituting two threonines (underlined in the sequence that follows) without altering the amino acid sequence of Vp2/3. The sense primers, 5'-TAAAAGCTTACGAAGACGGCCCCAACAAAA(A/C)GAAAGGAAG-3' (nt 1490 to 1530), and the above-mentioned antisense primer were used with pSV40 as a template for PCR, and the resulting PCR fragments were digested with *HindIII-Bpu1102I* to obtain the 217-bp fragment. In the sense primer, the nucleotide sequence at the Vp3 lysine 202 (AAG) was degenerate, leading either to the original lysine or to a threonine substitution. In order to facilitate the use of the *AccI* site within the SV40 sequence, the *AccI/SalI* site within pBR322 (nt 651) of both constructs was destroyed to yield pSV40- $\Delta$ Vp1Met $\Delta$ SalI and pSV40-Vp2/3<sub>202T</sub>- $\Delta$ Vp1Met $\Delta$ SalI, respectively, by digestion with *SalI*, followed by circularization after the repair reaction of the cleaved ends. *BamHI* linker (5'-pCGGATCCG-3'; New England Biolabs) was inserted at the single *AccI* site of SV40 following the repair reaction. Finally, pSV-Vp2/3 and pSV-Vp2/3<sub>202T</sub> were constructed by the removal of the 0.9-kb *BamHI* fragment containing the Vp1 coding sequence.

NO-pSV40 and NO-pSV40-Vp2/3<sub>202T</sub> were constructed from pSV40- $\Delta$ Vp1Met $\Delta$ SalI and pSV40-Vp2/3<sub>202T</sub>- $\Delta$ Vp1Met $\Delta$ SalI, respectively, by inserting an *XbaI* linker (5'-pCTCTAGAG-3'; New England Biolabs) at the *AccI* site. The *XbaI-SacI* fragment from pSV-Vp1, containing the full-length Vp1 coding sequence, was inserted into the *XbaI* and *SacI* sites to generate NO-pSV40 and NO-pSV40-Vp2/3<sub>202T</sub>.

NO-pSV40-Vp1 $\Delta$ N5 and NO-pSV40-Vp2/3<sub>202T</sub>-Vp1 $\Delta$ N5

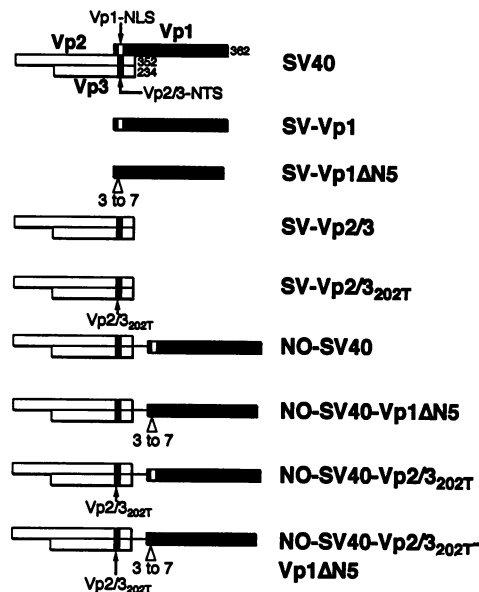


FIG. 2. Late gene structure of the variant SV40 DNAs. The Vp2/3 (□) and Vp1 (■) genes are indicated. Vp1 and Vp2/3 nuclear targeting signals are marked (arrows) as open and solid segments, respectively, within each of the coding sequences. The Vp2/3<sub>202T</sub> mutation is indicated as a white vertical line within the nuclear targeting signal, and the Vp1ΔN5 deletion is indicated by an open arrowhead below the nuclear targeting signal. The numbers adjacent to the coding sequences indicate the last amino acid.

were generated by exchanging the *Xba*I-*Sac*I fragments with those derived from pSV-Vp1ΔN5.

All constructions were verified by dideoxynucleotide double-stranded plasmid sequencing with Sequenase version 2.0 (United States Biochemical). Oligonucleotides for PCR were synthesized by the Preparation Laboratory of the UCLA Molecular Biology Institute.

**Cells, microinjection, and plaque assay.** Culture conditions for TC7 cells, a subline of African green monkey kidney epithelial cells, and microinjection procedures have been described previously (7). The derivatives of SV40 DNAs for microinjection were obtained by digesting the plasmids at *Bam*HI sites to eliminate the pBR322 region and recircularizing the DNAs (3.3 μg/ml) with T4 DNA ligase (16.7 U/ml). After the ligation reaction, the DNAs were concentrated with a Centricon 30 microconcentrator (Amicon), phenol-chloroform extracted, ethanol precipitated, and resuspended in phosphate-buffered saline at a concentration of 50 ng/μl. DNAs were microinjected into the nucleus of TC7 cells which were grown on coverslips marked for easy location of injected cells. At this concentration, each cell is expected to receive about 100 DNA molecules. For immunofluorescence studies, 100 to 200 cells were microinjected with each of the DNAs on the same coverslips and each experiment was repeated at least twice. The procedure for the plaque assay has been described previously (32).

**Indirect immunofluorescence.** The rabbit and guinea pig antisera against purified Vp3 and Vp1 have been described previously (8, 18). After the indicated incubation period, the microinjected cells were fixed in methanol-acetone (1:1) at -20°C, and stained first with hamster anti-large T antigen (1:50), guinea pig anti-Vp1 (1:50), and rabbit anti-Vp3 (1:50) and then with fluorescein isothiocyanate-, tetramethylrhoda-

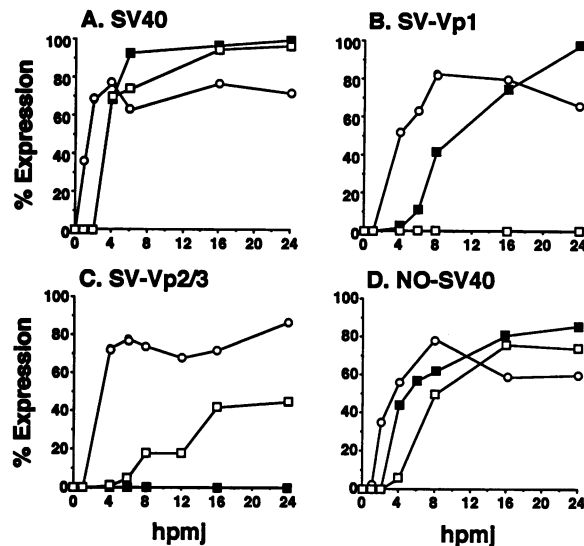


FIG. 3. Time course for the appearance of large T antigen, Vp1, and Vp2/3 in the variant DNA-injected cells. TC7 cells were microinjected with SV40 DNA (A), SV-Vp1 (B), SV-Vp2/3 (C), or NO-SV40 (D), incubated, and fixed at the indicated times (hpmj). Proteins were visualized by staining first with hamster anti-large T, guinea pig anti-Vp1, and rabbit anti-Vp3 antibodies and then with fluorescein isothiocyanate-goat anti-hamster IgG, tetramethylrhodamine isothiocyanate-goat anti-guinea pig IgG, and cascade blue-conjugated goat anti-rabbit IgG. Percent expression represents either the percentage of T-antigen-positive cells as a fraction of cells exhibiting large T-antigen staining (○) in total injected cells or the percentage of Vp1- or Vp3-positive cells as a fraction of cells exhibiting either Vp1 (■) or Vp3 staining (□) among large-T-antigen-positive cells.

mine isothiocyanate-, and cascade blue-conjugated goat secondary immunoglobulin Gs (IgGs) (1:50), respectively. In the triple-antigen detection procedure, we sometimes noted that the Vp3 cascade blue staining was difficult to unambiguously distinguish from the T-antigen fluorescein staining. The subcellular localization of the viral proteins was ascertained by the indirect immunofluorescent procedure using anti-Vp1 and anti-Vp3 (see the legends of Fig. 4 and 5). Washed coverslips were mounted onto glass slides and examined by fluorescence microscopy as described previously (7).

## RESULTS

**Construction of SV40 and its variant plasmids.** The structures of the late genes of SV40 and the variant DNAs used in this study are diagrammed in Fig. 2. All constructs harbor both large T-antigen and small t-antigen genes, regulatory elements, and an intact *agno* gene. SV40 variant plasmids pSV-Vp1 or pSV-Vp2/3 contain only one structural gene, Vp1 or Vp2/3, respectively, and pSV-Vp1ΔN5 and pSV-Vp2/3<sub>202T</sub> carry mutations in their nuclear targeting signals. In SV-Vp1ΔN5, the 3rd through 7th amino acids (Pro-Thr-Lys-Arg-Lys) of Vp1 which constitute the Vp1 NLS were deleted. pSV-Vp2/3 and pSV-Vp2/3<sub>202T</sub>, which contains a threonine substitution at Vp3 lysine 202 and has been shown to be critical for nuclear localization, lack the Vp1 coding sequence because ATG initiating codons in the Vp1 reading frame were mutated. A nonoverlapping SV40 variant plasmid, NO-pSV40, was also made to separate Vp2/3 and Vp1 coding sequences with a short spacer region between the two coding segments. Nuclear targeting signal mutations in Vp1 and/or Vp2/3 were intro-

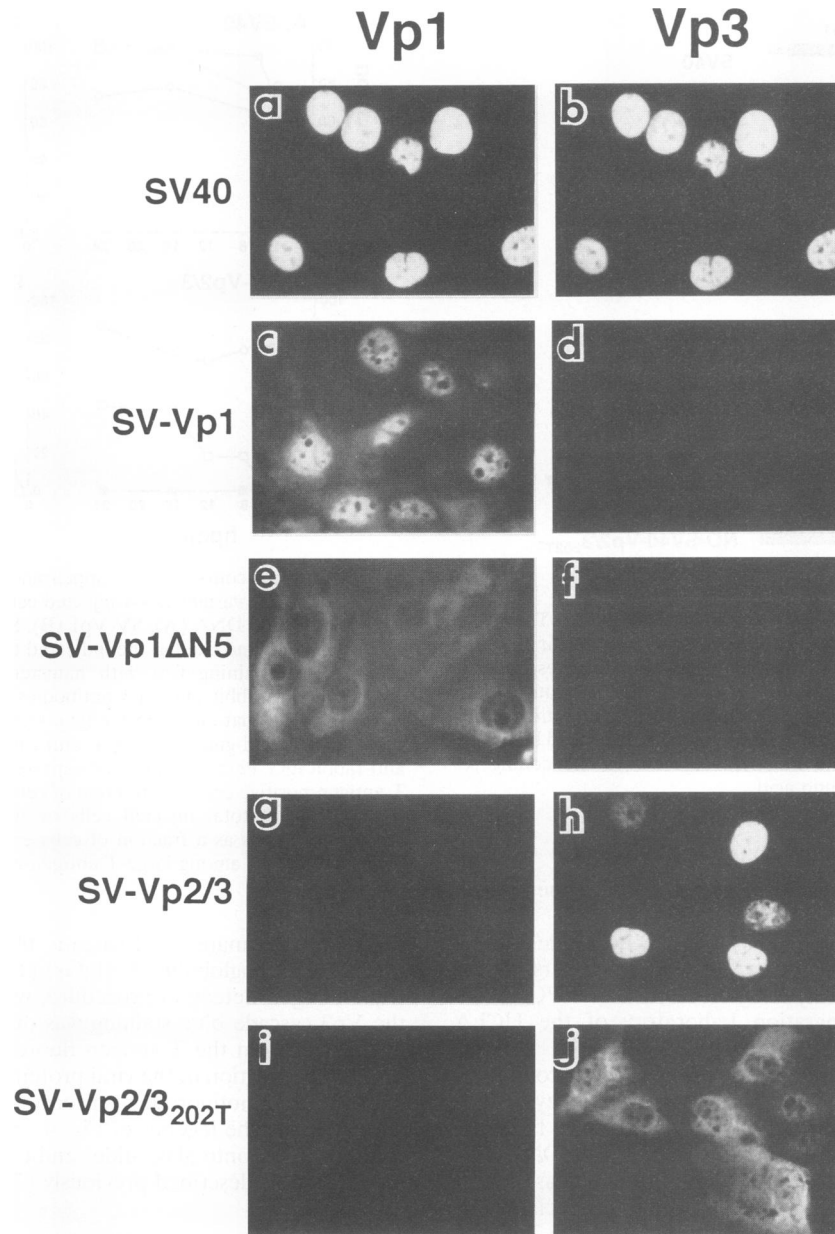


FIG. 4. Subcellular localization of singularly expressed capsid proteins. Cells were microinjected with plasmid-derived SV40 DNA (a and b), SV-Vp1 (c and d), SV-Vp1 $\Delta$ N5 (e and f), SV-Vp2/3 (g and h), or SV-Vp2/3<sub>202T</sub> (i and j) as described in Materials and Methods. Cells were fixed 24 hpmj, doubly stained first with guinea pig anti-Vp1 and rabbit anti-Vp3 antibodies and then with tetramethylrhodamine isothiocyanate–goat anti-guinea pig IgG and cascade blue-conjugated goat anti-rabbit IgG. Panels a, c, e, g, and i represent anti-Vp1 staining, and panels b, d, f, h, and j represent anti-Vp3 staining of the corresponding field of cells.

duced to generate NO-SV40-Vp2/3<sub>202T</sub>, NO-SV40-Vp1 $\Delta$ N5, or NO-SV40-Vp2/3<sub>202T</sub>-Vp1 $\Delta$ N5.

**Time course for the viral gene products encoded by SV40 variant DNAs.** Recircularized SV40 DNA as well as its variant DNAs, SV-Vp1, SV-Vp2/3, and NO-SV40, were microinjected into cells, and the appearance of large T antigen and the corresponding structural proteins was assessed cytochemically as a function of the time following injection (Fig. 3). In the SV40 DNA-injected cells, large T antigen was observed in most cells by 2 h postmicroinjection (hpmj), and Vp1 and Vp3 were observed by 4 to 5 hpmj (Fig. 3A). Most proteins were

observed to accumulate in the nucleus (see Fig. 4a and b and 7). Large T antigen expressed from the variant DNAs followed a time course similar to that of SV40, whereas the fraction of cells positive for Vp1 or Vp2/3 was variable, depending on the constructs (Fig. 3B, C, and D). In cells injected with SV-Vp1 or SV-Vp2/3, a proportion of either Vp1- or Vp2/3-positive cells reached a plateau level after 24 hpmj (Fig. 3B and C). Less than half of the T-antigen-positive cells in SV-Vp2/3-introduced cells showed Vp2/3 staining (Fig. 3C). Nonetheless, when the Vp1 or Vp2/3 staining was detectable at any given time point, all staining was found unambiguously in the

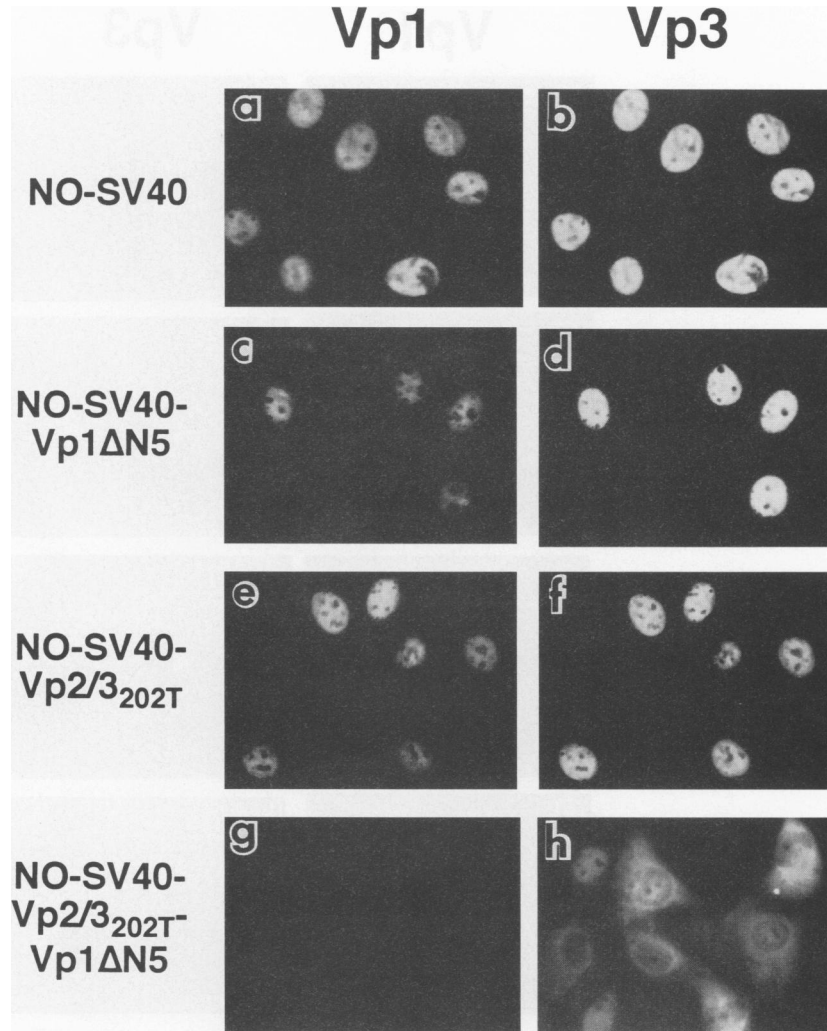


FIG. 5. Subcellular localization of capsid proteins expressed from NO-SV40 DNAs. Cells microinjected with NO-SV40 DNA (a and b), NO-SV40-Vp1 $\Delta$ N5 (c and d), NO-SV40-Vp2/3<sub>202T</sub> (e and f), or NO-SV40-Vp2/3<sub>202T</sub>-Vp1 $\Delta$ N5 (g and h) were processed at 24 hpmj as described in the legend to Fig. 4. Panels a, c, e, and g represent anti-Vp1 staining, and panels b, d, f, and h represent anti-Vp3 staining of the corresponding field of cells.

nucleus (Fig. 4c and h). No Vp2/3 or Vp1 was detected in SV-Vp1- or SV-Vp2/3-injected cells, respectively (Fig. 3B and C and 4d and g). NO-SV40 also showed efficient expression of large T antigen and the structural proteins, with Vp2/3 expression lagging behind that of Vp1 (Fig. 3D). On the basis of these observations, all analyses were performed at 24 hpmj in the following experiments.

**Vp2/3 and Vp1 nuclear targeting signals function in an interdependent manner.** The immunostaining patterns for the structural proteins in a field of cells are shown in Fig. 4, 5, and 6; and the distribution and subcellular localization of the individual proteins are summarized in Fig. 7. In SV-Vp1 (Fig. 4c and d)- and SV-Vp2/3 (Fig. 4g and h)-injected cells, the corresponding structural proteins efficiently localized to the nucleus (Fig. 7) as in SV40 DNA-injected cells (Fig. 4a and b), demonstrating that SV40 Vp1 and Vp2/3 contain their own nuclear targeting signals and are able to reach the nucleus independently. In SV-Vp1 $\Delta$ N5-injected cells, the truncated Vp1 $\Delta$ N5 protein was found in the cytoplasm (Fig. 4e and 7), as was the Vp2/3<sub>202T</sub> mutant protein in SV-Vp2/3<sub>202T</sub>-injected

cells (Fig. 4j and 7). The altered subcellular staining patterns in the cells expressing mutant proteins confirmed the importance of the N-terminal amino acid stretch of Vp1 (29) and the lysine 202 residue of Vp3 for their nuclear localization (7, 30).

To study how the independent Vp2/3 and Vp1 nuclear targeting signals encoded within the overlapping gene region cooperate with each other in the process of the nuclear targeting of viral proteins, we next constructed an NO-pSV40, in which the Vp2/3 and Vp1 genes are designed to be in tandem. NO-pSV40 DNA, following the removal of the plasmid DNA, was just as capable of plaque formation as SV40 DNA (data not shown). Using NO-SV40 and its variant DNAs, we examined the function of each signal in the presence of the corresponding counterpart structural protein. Vp1 and Vp3 expressed from NO-SV40 localized to the nucleus as expected (Fig. 5a and b and 7). While the mutant Vp2/3<sub>202T</sub> in SV-Vp2/3<sub>202T</sub>-injected cells was ineffective in nuclear targeting (Fig. 4j), it was effectively localized to the nucleus in the presence of full-length Vp1 (NO-SV40-Vp2/3<sub>202T</sub>) (Fig. 5f and 7). Likewise, the truncated Vp1 was effectively targeted to the nucleus

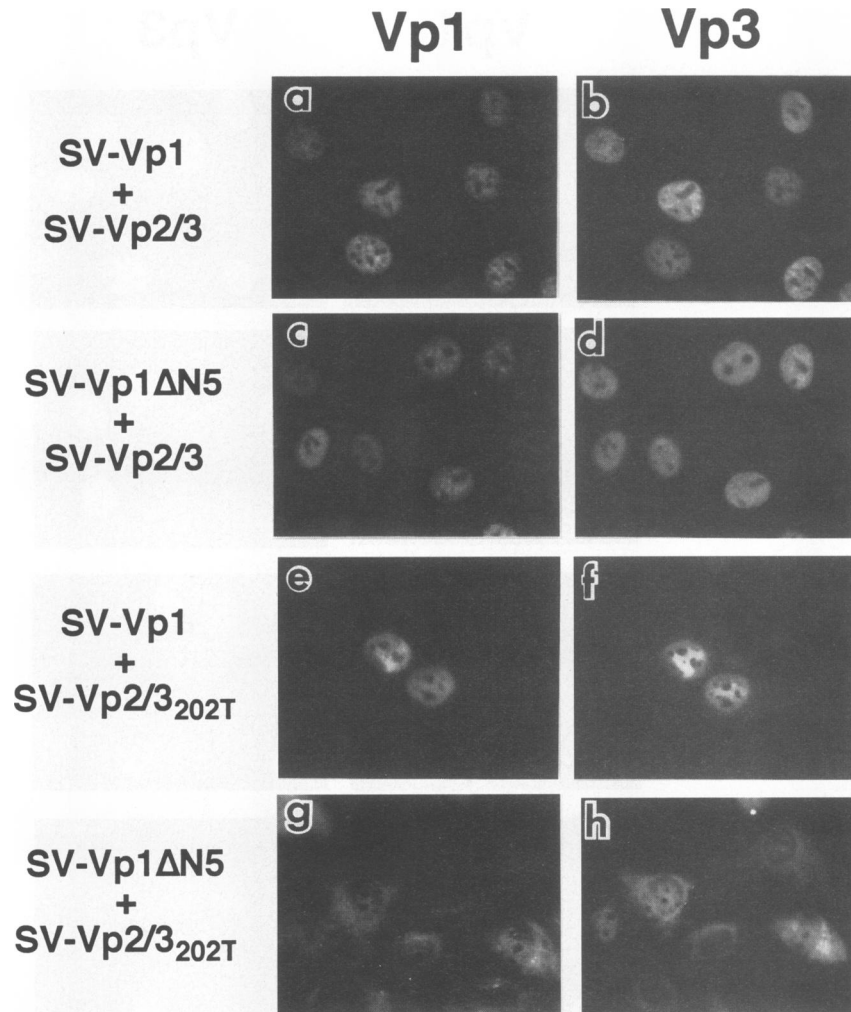


FIG. 6. Subcellular localization of Vp1 and Vp2/3 expressed from a combination of DNAs. Cells microinjected with SV-Vp1 and SV-Vp2/3 DNAs (a and b), SV-Vp1ΔN5 and SV-Vp2/3 (c and d), SV-Vp1 and SV-Vp2/3<sub>202T</sub> (e and f), or SV-Vp1ΔN5 and SV-Vp2/3<sub>202T</sub> (g and h) were processed at 24 hpmj as described in the legend to Fig. 4. Panels a, c, e, and g represent anti-Vp1 staining, and panels b, d, f, and h represent anti-Vp3 staining of the corresponding field of cells.

in the presence of Vp2/3 (Fig. 5c and 7), although the mutant Vp1 alone could only partially localize to the nucleus (Fig. 4e and 7). A similar complementation was observed when a combination of DNAs, SV-Vp1ΔN5 and SV-Vp2/3 (Fig. 6c and d and 7) or SV-Vp1 and SV-Vp2/3<sub>202T</sub> (Fig. 6e and f and 7), was introduced into the cells, and the subcellular localization of the mutant viral proteins was indistinguishable from that seen in cells in which the wild-type Vp1 gene and wild-type Vp2/3 gene were coexpressed (Fig. 6a through f). Thus, the nuclear targeting defect in one structural protein was complemented by the presence of another structural protein.

In the double mutant (NO-SV40-Vp2/3<sub>202T</sub>-Vp1ΔN5)-injected cells, the Vp2/3-NTS mutation maintained the SV-Vp2/3<sub>202T</sub> phenotype (Fig. 7) and showed cytoplasmic and perinuclear fluorescence (Fig. 5h). The truncated Vp1 was not observed in any compartment of the microinjected cells (Fig. 5g and 7). When the time course for the appearance of large T antigen, Vp2/3, and Vp1 was monitored in the double mutant-introduced cells, large T antigen and mutant Vp2/3, but not Vp1, were clearly detected up to 24 hpmj (data not shown). When the two SV40 variant DNAs, SV-Vp1ΔN5 and SV-Vp2/3

3<sub>202T</sub>, were coinjected, both mutant proteins were observed primarily in the cytoplasm (Fig. 6g and h and 7). Thus, the absence of Vp1ΔN5 in the double mutant-injected cells appears to reflect a repression of Vp1 synthesis when the two genes are contiguous on the same DNA molecule.

## DISCUSSION

In this study, the interrelationship of the nuclear targeting signals of SV40 structural proteins Vp1, Vp2, and Vp3 was tested by using variant SV40s in which only one of the structural proteins was present or by using a NO-SV40 in which the genes for Vp1 and Vp2/3 are separated. NO-SV40 expressed large T antigen, Vp1, and Vp2/3, produced a plaque, and thus could complete a lytic cycle. In the variant SV40 DNAs, the nuclear targeting signal-defective mutant protein Vp2/3<sub>202T</sub> or Vp1ΔN5, when expressed alone, remained in the cytoplasm but when a wild-type copy of the other structural protein was supplied and expressed, either in *cis* or in *trans*, the mutant protein then localized to the nucleus. These results demonstrate that while the nuclear targeting signal determines

the subcellular localization of each protein and is responsible for the protein nuclear localization following its synthesis in the cytoplasm, a functional defect of the signal in one capsid protein can be complemented by supplying the other capsid protein carrying an intact signal. The presence of at least one functional signal in *cis* or *trans* is essential for the observed complementation. These results suggest that additional signals such as those mediating the protein-protein interactions play a concerted role along with the nuclear targeting signal during SV40 morphogenesis. In the study presented here, we used anti-Vp3 which recognizes both Vp2 and Vp3 (18); thus, to what extent the Vp3 staining represents Vp2 molecules in which 118 residues unique to Vp2 including myristylated glycine (27) at its amino terminus cannot be evaluated.

There are a number of ways in which specific proteins can accumulate in the nucleus. The nuclear accumulation of proteins harboring nuclear targeting signals has been well documented (11). Proteins containing functionally weak signals can effectively localize to the nucleus when more than a few signals are present, as reported for the weakly active SV40 large-T-antigen NLS-pyruvate kinase fusion proteins (24), defective signals coupled to mouse IgG (20), or bovine serum albumin (12). Proteins containing no nuclear targeting signal have also been shown to localize to the nucleus if they interact with import-proficient shuttle proteins (for a review, see reference 14). For example, localization of the adenovirus DNA polymerase is facilitated by another viral protein, pTP (33), and NLS-deficient subfragments of hepatitis delta antigen can be transported into the nucleus by NLS-containing full-length antigens by complexing through leucine zipper sequences (31). Although the contribution of cooperative targeting by multiple signals and the piggyback transport to protein nuclear accumulation has been inferred (14), direct proof has been lacking. Our mutational analysis indicated that only one wild-type nuclear targeting signal of the two is sufficient for the piggyback targeting of SV40 proteins.

Reported evidence indicates that the host transport machineries appear to influence the nuclear targeting of viral proteins of polyomaviruses. Like SV40 structural proteins, Vp1 and Vp2/3 of related murine polyomavirus possess defined targeting signals that function in mammalian cells (3, 4). However, in insect cells, polyomavirus Vp2/3 was ineffectively targeted to the nucleus but became predominantly nuclear in the presence of polyomavirus Vp1 (10, 13). Because Vp1 effectively accumulated in the nucleus, Vp1-Vp2/3 interaction appears to mediate Vp2/3 nuclear localization. Since what was observed in host cells during infection by polyomaviruses (10, 13, 19, 22, 23, 26) does not reveal the role of individual protein components for nuclear targeting, these observations of insect cells (10, 13) as well as of CV-1 cells via vaccinia virus vector-expressed viral proteins (26) have been used to argue for a dominant role of Vp1 in nuclear targeting of Vp2/3 in polyomavirus infection (10, 13, 26). In this report, we have confirmed our earlier observation that SV40 Vp2/3 is able to reach the nucleus independently of Vp1 (7, 17). Currently, what causes this difference other than the difference in hosts in which the recombinant viral proteins are expressed is not known.

The experimental evidence presented here is in agreement with the hypothesis that the SV40 subviral assembly takes place in the cytoplasm (19, 22). A similar idea has recently been suggested for polyomavirus on the basis of protein-protein interaction studies (2) and results obtained by coexpression of polyomavirus Vp1 and Vp2/3 in mouse and insect cells (10, 13). What remains to be demonstrated is the identities of mutually interactive protein determinants and their role

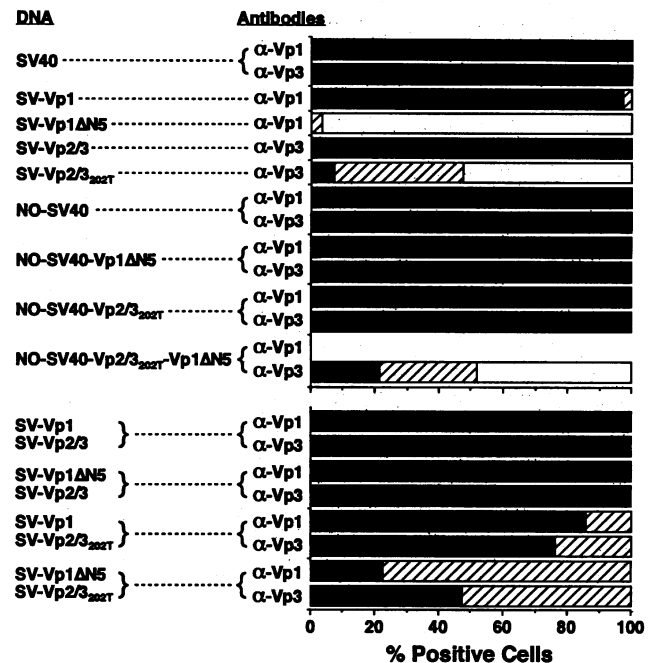


FIG. 7. Subcellular distribution of Vp1 and Vp2/3. Cells were injected with either individual variant DNAs or a combination of two variant DNAs as shown at the left. The number of cells exhibiting Vp1 or Vp2/3 (100%) was classified as N (■) or C (□), which showed distinct nuclear or cytoplasmic staining, respectively, and N>C (▨) or C>N (▩), in which staining was observed in both compartments with the staining predominantly in the nucleus or in the cytoplasm, respectively. Cells were processed as described in the legends to Fig. 4 to 6.

in the subviral assembly and protein nuclear targeting processes. Within the carboxyl 35 residues of SV40 Vp2/3, three signals, a Vp2/3 NTS, a Vp1-interactive determinant, and a DNA-binding domain, are present (6, 7, 15, 17, 30). In polyomavirus Vp2/3, a Vp2/3 NTS is at the carboxyl end (4) and a Vp1-interactive determinant has been recently mapped within residues 140 to 181 of the Vp3 (2). Polyomavirus Vp2/3 is shorter than SV40 Vp2/3 by 28 residues in which both a Vp1-interactive determinant and a DNA-binding domain of SV40 Vp2/3 are present. The location for the Vp1-interactive determinant of polyomavirus Vp3 raises a possibility that SV40 Vp3 has an additional domain that helps function in the protein-protein interaction with SV40 Vp1. Alternatively, the interactive determinant previously identified by deletion analysis (15) could have arisen from conformational change of the protein due to the truncation of the carboxyl 13 residues. The latter possibility has been suggested by Barouch and Harrison (2) on the basis of the amino acid homology found in residues between 170 and 181 of polyomavirus Vp3 and 174 and 185 of SV40 Vp3. This, however, is ruled out by results from our laboratory indicating that the Vp1-interactive determinant and the DNA-binding domain of Vp2/3, both of which occupy the last 13 residues of Vp2/3, are functionally separable from each other. Mutants that greatly impair DNA-binding activity can still interact with Vp1 (8a). Although the Vp2/3-interactive determinant of Vp1 has not been identified, it excludes residues 3 to 7 of Vp1, whose deletion resulted in the loss of nuclear targeting, but was complemented by Vp2/3 presumably through the protein-protein interaction. We can learn how additional signals defining the protein-protein interaction con-

tribute to the nuclear targeting of virion proteins when the Vp2/3-interactive determinant of Vp1 is identified.

An intriguing observation was that when the NO-SV40-Vp2/3<sub>202T</sub>-Vp1ΔN5 DNA was injected, the truncated Vp1 was not detected in any compartment of the cells (Fig. 5g and 7). Cytoplasmic Vp1ΔN5 and Vp2/3<sub>202T</sub> were detected in the same cells when the two genes on separate DNA molecules were coinjected (Fig. 6g). Thus, the observed Vp1 repression occurred when the two mutant genes were arranged in *cis*. Since NO-SV40 is viable, we assume that the amount of all structural proteins expressed in the NO-SV40 DNA-introduced cell is comparable to that in the normal SV40 DNA-introduced cell. Whether the reduced level of mutant Vp1 observed in the double mutant-injected cells reflects an experimental artifact or a regulatory role of Vp2/3 in Vp1 production remains to be tested.

#### ACKNOWLEDGMENTS

We are grateful to John N. Brady for supplying hamster anti-SV40 antiserum and to Eric Y. Chen and Andres L. Medina for assistance in some of the steps of plasmid construction. We also thank Arnold J. Berk and David A. Dean for critical reading of the manuscript.

This work was supported by Public Health Service grant CA50574 and in part by funds provided by the Committee on Research of the Academic Senate of the University of California, Los Angeles.

#### REFERENCES

- Baker, T. S., J. Drak, and M. Bina. 1988. Reconstruction of the three-dimensional structure of simian virus 40 and visualization of the chromatin core. *Proc. Natl. Acad. Sci. USA* **85**:422-426.
- Barouch, D. H., and S. C. Harrison. 1994. Interactions among the major and minor coat proteins of polyomavirus. *J. Virol.* **68**:3982-3989.
- Chang, D., J. I. Haynes, J. N. Brady, and R. A. Consigli. 1992. The use of additive and subtractive approaches to examine the nuclear localization sequence of the polyomavirus major capsid protein VP1. *Virology* **189**:821-827.
- Chang, D., J. I. Haynes, J. N. Brady, and R. A. Consigli. 1992. Identification of a nuclear localization sequence in the polyomavirus capsid protein VP2. *Virology* **191**:978-983.
- Chelsky, D., R. Ralph, and G. Jonak. 1989. Sequence requirements for synthetic peptide-mediated translocation to the nucleus. *Mol. Cell. Biol.* **9**:2487-2492.
- Clever, J., D. A. Dean, and H. Kasamatsu. 1993. Identification of a DNA binding domain in simian virus 40 capsid proteins Vp2 and Vp3. *J. Biol. Chem.* **268**:20877-20883.
- Clever, J., and H. Kasamatsu. 1991. Simian virus 40 Vp2/3 small structural proteins harbor their own nuclear transport signal. *Virology* **181**:78-90.
- Clever, J., M. Yamada, and H. Kasamatsu. 1991. Import of simian virus 40 virions through nuclear pore complexes. *Proc. Natl. Acad. Sci. USA* **88**:7333-7337.
- Dean, D. A., et al. Unpublished data.
- Dean, D. A., and H. Kasamatsu. 1994. Signal- and energy-dependent nuclear transport of SV40 Vp3 by isolated nuclei: establishment of a filtration assay for nuclear protein import. *J. Biol. Chem.* **269**:4910-4916.
- Delos, S. E., L. Montross, R. B. Moreland, and R. L. Garcea. 1993. Expression of the polyomavirus VP2 and VP3 proteins in insect cells: coexpression with the major capsid protein VP1 alters VP2/VP3 subcellular localization. *Virology* **194**:393-398.
- Dingwall, C., and R. A. Laskey. 1992. The nuclear membrane. *Science* **258**:942-947.
- Dworetzky, S. I., R. E. Lanford, and C. M. Feldherr. 1988. The effects of variations in the number and sequence of targeting signals on nuclear uptake. *J. Cell Biol.* **107**:1279-1287.
- Forstová, J., N. Krauzewicz, S. Wallace, A. J. Street, S. M. Dilworth, S. Beard, and B. E. Griffin. 1993. Cooperation of structural proteins during late events in the life cycle of polyomavirus. *J. Virol.* **67**:1405-1413.
- Garcia-Bustos, J., J. Heitman, and M. N. Hall. 1991. Nuclear protein localization. *Biochim. Biophys. Acta* **1071**:83-101.
- Gharakhanian, E., and H. Kasamatsu. 1990. Two independent signals, a nuclear localization signal and a Vp1-interaction signal, reside within the carboxy-35 amino acids of SV40 Vp3. *Virology* **178**:62-71.
- Gharakhanian, E., J. Takahashi, J. Clever, and H. Kasamatsu. 1988. *In vitro* assay for protein-protein interaction: carboxyl-terminal 40 residues of simian virus 40 structural protein Vp3 contain a determinant for interaction with Vp1. *Proc. Natl. Acad. Sci. USA* **85**:6607-6611.
- Gharakhanian, E., J. Takahashi, and H. Kasamatsu. 1987. The carboxyl 35 amino acids of SV40 Vp3 are essential for its nuclear accumulation. *Virology* **157**:440-448.
- Kasamatsu, H., and A. Nehorayan. 1979. Intracellular localization of viral polypeptides during simian virus 40 infection. *J. Virol.* **32**:648-660.
- Kasamatsu, H., and A. Nehorayan. 1979. Vp1 affects intracellular localization of Vp3 polypeptide during simian virus 40 infection. *Proc. Natl. Acad. Sci. USA* **76**:2808-2812.
- Lanford, R. E., C. M. Feldherr, R. G. White, R. G. Dunham, and P. Kanda. 1990. Comparison of diverse transport signals in synthetic peptide-induced nuclear transport. *Exp. Cell Res.* **186**:32-38.
- Liddington, R. C., Y. Yan, J. Moulai, R. Sahli, T. L. Benjamin, and S. C. Harrison. 1991. Structure of simian virus 40 at 3.8-Å resolution. *Nature (London)* **354**:278-284.
- Lin, W., T. Hata, and H. Kasamatsu. 1984. Subcellular distribution of viral structural proteins during simian virus 40 infection. *J. Virol.* **50**:363-371.
- Lin, W., J. L. Shurgot, and H. Kasamatsu. 1986. The synthesis and transport of SV40 structural proteins. *Virology* **154**:108-120.
- Roberts, B. L., W. D. Richardson, and A. E. Smith. 1987. The effect of protein context on nuclear location signal function. *Cell* **50**:465-475.
- Sambrook, J., E. F. Fritsch, and T. Maniatis. 1989. *Molecular cloning: a laboratory manual*, 2nd ed. Cold Spring Harbor Laboratory, Cold Spring Harbor, N.Y.
- Stamatos, N. M., S. Chakrabarti, B. Moss, and J. D. Hare. 1987. Expression of polyomavirus virion proteins by a vaccinia virus vector: association of VP1 and VP2 with the nuclear framework. *J. Virol.* **61**:516-525.
- Streuli, C. H., and E. Griffin. 1987. Myristic acid is coupled to a structural protein of polyoma virus and SV40. *Nature (London)* **329**:619-622.
- Tooze, J. (ed.). 1981. *DNA tumor viruses*. Cold Spring Harbor Laboratory, Cold Spring Harbor, N.Y.
- Wychowski, C., D. Benichou, and M. Girard. 1986. A domain of SV40 capsid polypeptide VP1 that specifies migration into the cell nucleus. *EMBO J.* **5**:2569-2576.
- Wychowski, C., D. Benichou, and M. Girard. 1987. The intranuclear location of simian virus 40 polypeptides VP2 and VP3 depends on a specific amino acid sequence. *J. Virol.* **61**:3862-3869.
- Xia, Y.-P., C.-T. Yeh, J.-H. Ou, and M. M. C. Lai. 1992. Characterization of nuclear targeting signal of hepatitis delta antigen: nuclear transport as a protein complex. *J. Virol.* **66**:914-921.
- Yamada, M., and H. Kasamatsu. 1993. Role of nuclear pore complex in simian virus 40 nuclear targeting. *J. Virol.* **67**:119-130.
- Zhao, L.-J., and R. Padmanabhan. 1988. Nuclear transport of adenovirus DNA polymerase is facilitated by interaction with preterminal protein. *Cell* **55**:1005-1015.